Communication

Imaging Chirality with Surface Second Harmonic Generation Microscopy

Matthew A. Kriech, and John C. Conboy

J. Am. Chem. Soc., **2005**, 127 (9), 2834-2835• DOI: 10.1021/ja0430649 • Publication Date (Web): 08 February 2005

TOCG

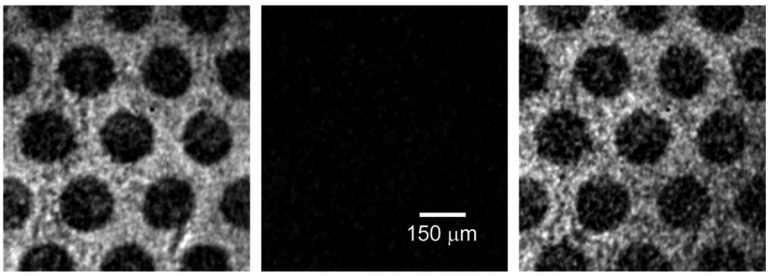

More About This Article

Additional resources and features associated with this article are available within the HTML version:

- Supporting Information
- Links to the 1 articles that cite this article, as of the time of this article download
- Access to high resolution figures
- Links to articles and content related to this article
- Copyright permission to reproduce figures and/or text from this article

View the Full Text HTML

J|A|C|S
COMMUNICATIONS

Published on Web 02/08/2005

Imaging Chirality with Surface Second Harmonic Generation Microscopy

Matthew A. Kriech and John C. Conboy*

Department of Chemistry, University of Utah, 315 S. 1400 E. RM 2020, Salt Lake City, Utah 84112

Received November 17, 2004; E-mail: conboy@chem.utah.edu

Chirality is a fundamental construct in nature which arises from an antisymmetric arrangement of atoms, molecules, or larger structures, resulting in the formation of nonsuperimposable mirror images.[1] Bulk chiral effects can easily be measured using circular dichroism (CD) or optical rotary dispersion (ORD).[1] However, the quantification of chirality for molecular surface films cannot be obtained with these linear spectroscopic methods.

Not surprisingly, the direct optical imaging of chirality originating from a planar surface film has proven to be a challenging problem. The ability to image chirality on a surface has been accomplished on the molecular scale using atomic force microscopy (AFM)[2−4] and scanning tunneling microscopy (STM),[2,5−7] where chirality is inferred from the two-dimensional antisymmetric arrangement of atoms or groups of atoms to form extended chiral structures.

Optical microscopies based on the preferential absorbance of right versus left circularly polarized light have been used to image chiral structures in bulk crystals.[8] However, no direct image of chirality from a molecular surface film has ever been obtained with optical methods due to the limited path length and relatively weak nature of the CD or ORD response.

To overcome these limitations, we have developed the first nonlinear chiral microscope. Using second harmonic generation (SHG), with its inherent surface sensitivity and ability to discriminate between the symmetry of surface adsorbed species,[9] in combination with a counter-propagating optical geometry,[10] we have obtained the first optical image originating solely from the intrinsic chirality of a surface film.

SHG is an established analytical tool that has been used extensively to study a variety of surfaces and interfaces.[9,11−13] SHG is a second-order nonlinear optical spectroscopy that arises when an optical field of sufficient intensity at frequency ω is directed at a surface, resulting in the generation of a second optical field at twice the frequency, 2ω.[9] SHG can only be observed when there is a break in inversion symmetry and is thus prohibited in the bulk of centrosymmetric materials, making the technique extremely well suited for the analysis of interfaces. Hicks et al. pioneered the use of SHG for investigating molecular chirality on surfaces by utilizing methods similar to CD and ORD.[14,15]

Confocal SHG microscopy has been widely applied to the imaging of bulk structures in biological systems.[16] The chiral structure of proteins and sugar modified dyes have been used, in particular, to enhance the SHG emission in biological membranes and tissues, facilitating imaging.[16,17] However, the direct visualization of chirality in a surface film is not possible with confocal SHG microscopy due to the geometry used to excite the sample.

We previously demonstrated that, by employing a counterpropagating SHG geometry, where the two photons strike the surface from opposite directions, the chiral emission from the surface can be isolated directly with high sensitivity and with the use of linearly polarized light.[10,18] SHG imaging[19−21] can also be performed in this geometry and has several advantages over a confocal arrangement for the imaging of chirality. By employing a counterpropagating geometry, the generated SHG photons are emitted along the surface normal. The chiral SHG (C-SHG) signal can be retrieved directly by selecting the *x*-polarized component of the emission. The intensity of the C-SHG emission is given by eq 1, and is a function of the incident angle (θ_i) and polarization state of the incident field ($\gamma = 0°$ is *p*-polarized and $\gamma = 90°$ is *s*-polarized), the chiral tensor element (χ_{xyz}), and the geometric Fresnel coefficients for the incident fields (f_y and f_z), with K representing the sum of the phase shifts for *p*- and *s*-polarized light upon reflection.[10]

$$I_{\mathrm{C-SHG}} = I_x = 64\pi^2 \sin^2(\theta_i) \sin^2(\gamma) \cos^2(\gamma) f_y^2 f_z^2 \chi_{xyz}^2 K^2 \quad (1)$$

From eq 1 it can be seen that the C-SHG response for a counterpropagating geometry is simply a function of the second-order chiral susceptibility tensor, χ_{xyz}, with a maximum in $I_{\mathrm{C-SHG}}$ occurring with a mixed polarization state of the incident fields ($\gamma = 45°$). The measured C-SHG light intensity is directly proportional to the "amount" of chirality on the surface. By reconstructing a spatial image of the emitted photons, using a microscope objective, an image of surface chirality can be generated. This technique has the advantage of fluorescent microscopy, but unlike fluorescence no fluorescent label is required for visualization, instead the intrinsic chirality of the molecule can be used as a label-free probe.

In the study presented here, the intrinsic chirality of *R*- and *S*-(+)-1,1′-bi-2-naphthol (RBN, SBN) has been used to image a patterned planar supported lipid bilayer (PSLB) using C-SHG. RBN and SBN were chosen due to their low molecular weight, lack of intrinsic fluorescence, and their strong chiral response in the UV region. Poly(dimethylsiloxane) (PDMS) stamps were used to create a series of alternating holes in a fluid PSLB by microcontact printing (μCP). The patterned PSLB was maintained in an aqueous environment and mounted on an optical flow cell for imaging. Solutions (17.3 μM) of RBN, SBN, and a racemic mixture of RBN and SBN were injected above the μCP PSLB and allowed to equilibrate for 20 min prior to obtaining an image. RBN and SBN exchange freely between solution and a lipid membrane allowing for easy exchange of enantiomers in the membrane.

The nonlinear chiral microscope used in these studies consisted of a OPOTEK optical parametric oscillator which was pumped with a 10 Hz Nd:YAG laser (Continuum) with a 7 ns pulse duration. The sample was excited at 520 nm, with detection of the C-SHG light at 260 nm. Imaging of the C-SHG emission was performed with a modified Olympus microscope with a UV 10× objective (Optics for Research). A solar blind image intensifier (Phototek) which was lens coupled to a CCD camera (Roper Scientific) was used for image collection. A 30 min integration time was used to acquire the C-SHG images.

An example of a C-SHG micrograph is given in Figure 1a, where the emission from RBN intercalated into a patterned PSLB of 1-palmitoyl-2-oleoyl-*sn*-glycero-3-phosphocholine (POPC) is shown. The image has been flat-field corrected to account for the nonuniformity in the excitation field. The bright regions in the

 10.1021/ja0430649 CCC: $30.25

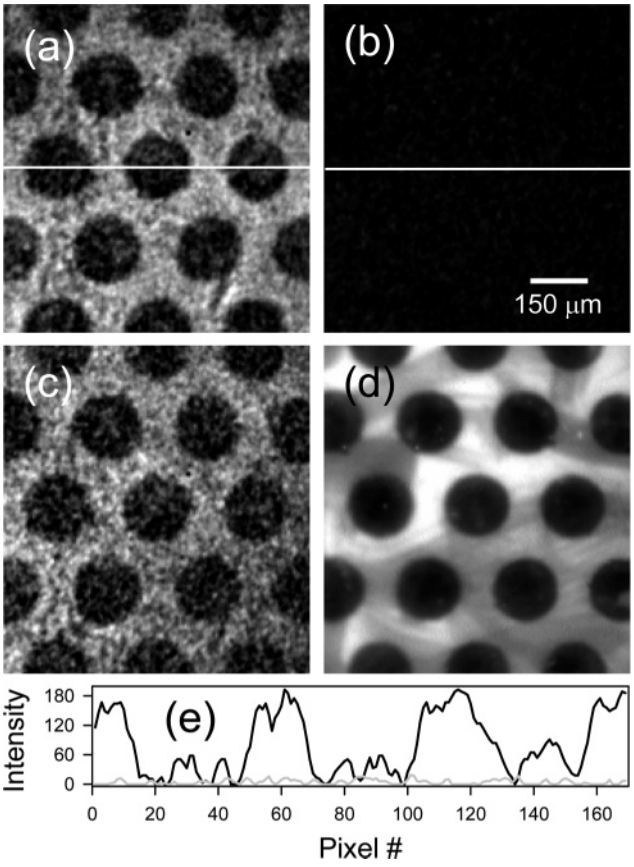

Figure 1. A μCP POPC PSLB imaged with C-SHG using (a) RBN, (b) a racemic mixture of RBN and SBN, and (c) SBN. A different bilayer was also imaged with Rh-DOPE using fluorescence microscopy (d). Line scans through the center of image a (black) and b (gray) are shown in part e.

C-SHG image correspond to regions in which RBN has intercalated in the membrane, while the dark regions correspond to voids in the lipid film which have been removed by μCP. Since RBN does not bind to bare silica, no chiral emission is observed. To demonstrate that the C-SHG imaging technique is sensitive to the chiral species at the surface, a racemic mixture of RBN and SBN was also injected above the membrane surface, Figure 1b. Since equal numbers of each enantiomer are now bound within the membrane, the net result is a cancellation in the overall C-SHG emission. The alternating pattern within the membrane is no longer visible due to the absence of surface chirality. To prove the patterned membrane still remains, a solution of SBN was subsequently injected over the same POPC bilayer, resulting in the restoration of the C-SHG image, Figure 1c, due to the presence of a single enantiomer in the membrane.

Figure 1e shows a line scan through the center of Figure 1a and b. The large intensity difference in the measured C-SHG emission between the voids in the μCP PSLB and the intact membrane is clearly visible. The line scan for the racemic mixture shows little or no intensity with no variation throughout the membrane, verifying that the intrinsic chirality of RBN and SBN is responsible for generating the image of the patterned membrane.

For comparison, a fluorescence micrograph of a μCP PSLB was obtained by incorporating the ammonium salt of 1,2-dioleoyl-*sn*-glycero-3-phosphoethanolamine-*N*-[lissamine rhodamine B sulfonyl] (Rh-DOPE, Avanti Polar Lipids) at 4 mol % into the bilayer during the deposition, Figure 1d. Excellent agreement between the C-SHG and the fluorescence image is obtained. The dark circles, which are approximately 150 μm in diameter, are identical to those observed by C-SHG. The bright regions are where the membrane remains and contains Rh-DOPE.

The ability to retrieve spatial information on surface chirality, as demonstrated in Figure 1, cannot be achieved with conventional linear optical methods. C-SHG, however, possesses the requisite surface selectivity and sensitivity to detect interfacial chirality and provides a direct route for the visulization of chirality originating from molecluar surface films. C-SHG imaging introduces the possibility of observing protein domains in cell membranes and chiral structures in monolayer films directly. A C-SHG imaging system also has certain advantages over conventional fluorescent microscopy, most importantly the label-free nature of the C-SHG technique. Instead of fluorescently tagging a target molecule, the intrinsic chirality of a molecule can be used as a label-free probe.

We have demonstrated here for the first time that C-SHG can be used as a powerful imaging technique for the detection of molecular chirality at a surface. Studies are ongoing to adapt chiral imaging for the label-free measurement of protein and DNA binding in microarray-based assays. The label-free nature of C-SHG imaging is also being applied to the study of localized protein structures in membranes and extended chiral structures in monolayer films.

Acknowledgment. The authors would like to thank Mr. Dennis Romney and Mr. Jeff Whelch for construction of the UV microscope. This work was supported by funds from the NIH (R01 GM068120-01).

Supporting Information Available: Detailed experimental description. This material is available free of charge via the Internet at http://pubs.acs.org.

References

(1) *Circular Dichroism and the Conformational Analysis of Biomolecules*; Plenum Press: New York, 1996.
(2) Hermann, B. A.; Hubler, U.; Guntherodt, H. J. *ACS Symposium Series* **2002**, *810*, 186−204.
(3) Huang, X.; Li, C.; Jiang, S.; Wang, X.; Zhang, B.; Liu, M. *J. Am. Chem. Soc.* **2004**, *126*, 1322−1323.
(4) France, C. B.; Parkinson, B. A. *J. Am. Chem. Soc.* **2003**, *125*, 12712−12713.
(5) Bohringer, M.; Morgenstern, K.; Schneider, W.-D.; Berndt, R. *Angew. Chem.* **1999**, *38*, 821−823.
(6) Cai, Y.; Bernasek, S. L. *J. Am. Chem. Soc.* **2003**, *125*, 1655−1659.
(7) Lopinski, G. P.; Moffatt, D. J.; Wayner, D. D. M.; Wolkow, R. A. *Nature* **1998**, *392*, 909−911.
(8) Claborn, K.; Puklin-Faucher, E.; Kurimoto, M.; Kaminsky, W.; Kahr, B. *J. Am. Chem. Soc.* **2003**, *125*, 14825−14831.
(9) Shen, Y. R. *The Principles of Nonlinear Optics*; Wiley: New York, 1984.
(10) Kriech, M. A.; Conboy, J. C. *J. Opt. Soc. Am. B* **2004**, *21*, 1013−1022.
(11) Conboy, J. C.; Daschbach, J. L.; Richmond, G. L. *J. Phys. Chem.* **1994**, 9688−9692.
(12) Corn, R. M. *Adsorpt. Mol. Met. Electrodes* **1992**, 391−408.
(13) Eisenthal, K. B. *Annu. Rev. Phys. Chem.* **1992**, *43*, 627.
(14) Byers, J. D.; Yee, H. I.; Hicks, J. M. *J. Chem. Phys.* **1994**, *101*, 6233−6241.
(15) Byers, J. D.; Yee, H. I.; Petralli-Mallow, T.; Hicks, J. M. *Phys. Rev. B* **1994**, *49*, 14643−14647.
(16) Campagnola, P. J.; Loew, L. M. *Nat. Biotechnol.* **2003**, *21*, 1356−1360.
(17) Campagnola, P. J.; Wei, M.-D.; Lewis, A.; Loew, L. M. *Biophys. J.* **1999**, *77*, 3341−3349.
(18) Kriech, M. A.; Conboy, J. C. *J. Am. Chem. Soc.* **2003**, *125*, 1148−1149.
(19) Ashida, T.; Yamamoto, Y.; Kurimura, S.; Uesu, Y. *Ferroelectrics* **1996**, *184*, 171−178.
(20) Florsheimer, M.; Bosch, M.; Brillert, C.; Wierschem, M.; Fuchs, H. *J. Vac. Sci. Technol., B* **1997**, *15*, 1564−1568.
(21) Smilowitz, L.; Jia, Q. X.; Yang, X.; Li, D. Q.; McBranch, D.; Robinson, J. M. *Mater. Res. Soc. Symp. Proc.* **1997**, *440*, 209−214.

JA0430649